Assessment of wave power variability and exploitation with a long-term hindcast database

Nicolas Guillou, Georges Chapalain

Version of Record: https://www.sciencedirect.com/science/article/pii/S0960148120304018
Manuscript_7544c163f9aa4525dcc50856e2bfa664

Assessment of wave power variability and exploitation with a long-term hindcast database

Nicolas Guillou[a,*], Georges Chapalain[a]

[a] *Cerema, Direction Eau Mer et Fleuves, Environnement et Risques, Laboratoire de Génie Côtier et Environnement (LGCE), 155 rue Pierre Bouguer, Technopôle Brest-Iroise, BP 5, 29280 Plouzané, France*

Abstract

Numerical investigations dedicated to the impact of wave power variability on energy conversion were mainly conducted in the European shelf seas where a considerable amount of technological devices was developed. We complemented these studies by exploiting a 31-year consistent hindcast database of the wave climate, assessed against observations in 41 locations, in the North-West Atlantic, the Gulf of Mexico and the Caribbean Sea. With an exception in the Caribbean Sea where wave power density increased under the influence of an easterly zonal wind, a clear contrast was exhibited between the oceanic energetic regions and the semi-enclosed basins. The analysis revealed furthermore contrasting wave climates characterized by (i) significant temporal variability in the Gulf of Mexico and the northern oceanic region off the USA East Coast, and (ii) more moderated variations in the Caribbean Sea off Colombia and the southern oceanic area off the Lesser Antilles. A generic method, independent from the device technology, was finally adopted

*Corresponding author
Email address: nicolas.guillou@cerema.fr (Nicolas Guillou)

to assess the effects of resource variability on energy output and converters performances. The area off the Lesser Antilles appeared particularly interesting to supply, at reduced installed capacity but with more regular waves conditions, renewable energy within surrounding island territories.
Keywords: wave energy converters, WWIII, numerical modeling, Gulf of Mexico, Caribbean Sea, North-West Atlantic.

---

1. Introduction

Whereas wave energy converters (WEC) are still in the early stages of development, the exploitation of the wave resource may be a solution to supply, in a near future, a part of renewable energy within the electricity grid of marine territories [1]. Wave energy is thus characterized by a high power density and may theoretically be exploited in many more potential locations than other marine resources such as tidal stream energy whose extraction is restricted to strong-currents areas like estuaries entrance or straits. However, the wave resource shows also significant seasonal and annual variabilities that may impact the performances, economical return and sitting of wave energy projects [2, 3]. Beyond the total amount of available power, the temporal variability of wave climate may influence the steadiness of expected power output with varying responses depending on the operational range of WEC power matrices [4]. In the most energetic locations primary targeted for the setup of wave energy projects, high temporal variability of the available resource may furthermore increase the construction costs of devices designed to withstand harsh environmental storm conditions, while reducing the economical reliability of the project [3]. Successful design and deployment of WEC in the marine environment require thus accurate assessments of the wave climate on multi-decadal periods of time. This will help to optimize the capital investment and adapt, in some cases, the technological options (modifying, for instance, the rated and maximum operating conditions of devices) [5].

A series of investigations based on numerical hindcast modeling were conducted to assess the variability of available wave power. As a considerable

number of technological devices was developed and tested in the northwest European shelf seas, the major part of wave power assessment focused on this environment by exhibiting the seasonal and annual variabilities of the available resource on a global scale [6], or at the scale of marine territories [7, 8, 9, 10]. Long-term assessments of wave power variability were also conducted in the most energetic areas around the world including the coasts of Canada [11] and Morocco [12], the Caribbean [13] and south China seas [14], or the Australian [15] and Brazilian shelf environments [16]. Whereas these numerical investigations, outside the European shelf seas, provided further very interesting insights about the temporal evolution of the available resource, the attention was focused on monthly and seasonal averaged spatial patterns setting aside further studies about its annual variability.

Following these resource assessments, particular attention was dedicated to the effects of wave power variability on WEC performances in the regions around the world with the highest wave power density (see [4] for a non-exhaustive review). However, besides being dependent from the device technology, most of the numerical investigations, conducted outside the European shelf seas, ignored these effects focusing on averaged expected power outputs. Reduced efforts were, in particular, devoted to assess the wave energy practically available for electricity conversion in locations with varying wave climate. These aspects appeared yet important to consider in the preliminary stages of a wave energy project. In a comparative study between the North Atlantic and the Equatorial Pacific, Portilla et al. [3] exhibited that less energetic, but with reduced variability and severe storm conditions, may have a technically exploitable resource comparable to the most energetic

locations traditionally considered in wave power characterization.

The present investigation complements the numerical evaluations of the wave energy climate conducted outside the European shelf seas by analyzing, at the regional and local scales, (i) the monthly, seasonal and annual variabilities of the available wave energy flux and (ii) the potential for power conversion of marine locations with varying energy levels. The application was conducted in the Gulf of Mexico (GoM), the Caribbean Sea (CS), and the North-West Atlantic Ocean characterized by different levels of available wave energy with semi-enclosed sea basins separated from the oceanic energetic conditions by a series of islands, which are typical energy-starved territories primary targeted for the setup of wave energy projects (Fig. 1). Beyond these local energy needs, the area of interest is also characterized by a very large electricity consumption associated with the urban and industrial plants disseminated along the coast of USA, and the very impressive number (over 3500) of oil and gas platforms in the GoM [17]. This study exploited a global consistent multi-decadal wave hindcast database, released in 2017 by the National Oceanic and Atmospheric Administration (NOAA) [18], exhibiting, for broader investigations, the benefits associated for the assessments of wave power variability in coastal seas around the world.

The paper is organized as follows. In Section 2, we described the study site providing further insights about previous numerical investigations of wave temporal variability. In Section 3, some details were successively given about the wave hindcast database, the computation of the available wave energy flux and the metrics retained to characterize the resource variability at monthly, seasonal and annual time scales. In Section 4.1, we assessed the

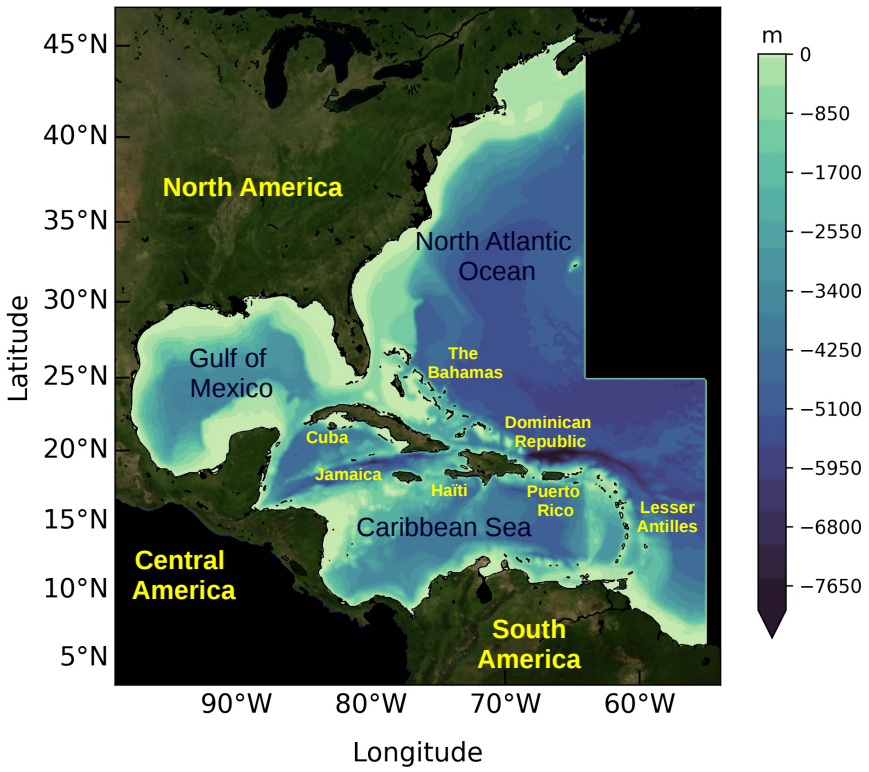

Figure 1: Bathymetry of the area of interest with the delimitation of WWIII computational domain.

reliability of the wave hindcast database by comparing predictions of wave power density with a series of medium and long-term observations in buoys of the National Data Buoy Center (NDBC) [19]. In Sections 4.2 and 4.3, we evaluated the spatial distributions of yearly and seasonal-averaged wave energetic patterns and characterized the temporal variability of available wave power at monthly, seasonal and annual time scales focusing on four locations with contrasting wave energy climate. In Section 4.4, we applied a generic method proposed by Portilla et al. [3] to compare the effects of resource

variability on energy output in these four locations. This application provided information, independent from the device technology, that may help developers to optimize energy converters in these environments. Conclusions and perspectives were finally drawn in Section 5.

2. Study site

The area of interest integrates the semi-enclosed basins of the Gulf of Mexico and the Caribbean Sea, and the eastern coastal and oceanic areas of North-West Atlantic Ocean (Fig. 1). Whereas the oceanic region is characterized by reduced available wave energy flux in comparison with the European shelf seas or the West Coast of USA [2], this environment integrates, along the shoreline, a significant amount of total accessible wave power estimated at 240 TWh par year [5]. The GoM and CS are separated from the energetic oceanic conditions by a series of islands including the Bahamas (in the south of Florida), the Greater Antilles (Cuba, Haïti, the Dominican Republic, and Puerto Rico...), and the Lesser Antilles that develop along the volcanic island arc between Puerto Rico and South America. This results in reduced wave energy potential estimated in the GoM at 80 TWh per year [5]. However, these semi-enclosed basins are subjected to extreme wind waves conditions including (i) mid-latitude anticyclonic systems with cold fronts and (ii) low pressure systems characterized by tropical cyclones (depressions, tropical storms and hurricanes) [20]. The frontal cold systems occur typically between December and March whereas the hurricane season takes mainly place between June and November [21]. In the past 150 years, more than one thousand tropical cyclones were recorded in the GoM [17].

The existence of cold fronts and tropical storms within these semi-enclosed basins increases thus the temporal variability of the wave climate with periods of moderate sea states succeeding extreme waves. The wave climate differs thus broadly between the coastal basins of GoM and CS, and the oceanic region.

Apart from worldwide numerical investigations [2, 22, 23], few studies were conducted in the area of interest to assess the temporal variability of the available wave energy potential. By analyzing NDBC wave stations observations, Defne et al. [24] assessed the monthly variability of the wave power potential along the southeastern Atlantic coast of the USA exhibiting a considerable accessible wave energy resource when integrated along the shoreline. By exploiting multi-decadal meteorological data provided by the NOAA, Haces-Fernandez et al. [25] characterized, with a new approach based on peak-over-threshold method, the spatial and temporal variability of the wave energy flux in three regions of the USA (inclusing the GoM, East and West Coasts). This analysis exhibited the differences in wave power density, with more energetic events along the USA East Coast than in the GoM, suggesting to adapt the WEC configuration to the different sea states. These investigations were complemented by local refined numerical modeling studies in the GoM and CS [13, 26], and along the USA East Coast [27]. However, with an exception for the analysis conducted by Appendini et al. [13] devoted to the southeastern part of CS, reduced effort was dedicated to investigate the temporal variability of the available wave power.

3. Materials and methods

3.1. Wave hindcast database

The wave hindcast database considered here was generated by the National Center for Environmental Prediction (NCEP) [28] with the NOAA Wavewatch III (WWIII) spectral wave model [29] that incorporated the physics package developed by Ardhuin et al. [30]. Further details about the physical and numerical parameterisations, and setup of the wave model are available in [28] and [31, 32]. In comparison with previous worldwide database maintained by the NCEP, waves predictions here obtained constitute a consistent multi-decadal database. The wave model was thus driven during 31 years, between 1979 and 2009, by the reanalysis of wind fields from the new NCEP Climate Forecast System Reanalysis Reforecast (CFSRR) covering the globe on an 0.5^{o} spatial and hourly temporal resolutions [33]. Simulations were performed on 16 computational grids with two-way-interaction between the higher and lower resolution domains. A spatial resolution of $1/6^{o}$ was thus reached in the area of interest with a discretization in 50 frequencies and 36 evenly distributed directional bins. The database provided finally output field parameters of the significant wave height H_s and the peak period T_p with a time step of 3 hours. This wave hindcast database was assessed by the NCEP against measurements of H_s and T_p in the area of interest. Further details about this assessment are available in [28].

3.2. Wave power computation

The available wave energy flux (also denominated the available wave power density or wave energy potential per unit crest, in Wm^{-1}) is an inte-

gral parameter of the wave spectrum that characterizes the amount of energy reaching a given location. It is computed as

$$P = \rho g \int_0^\infty c_g(f) E(f) df \tag{1}$$

where ρ is the density of sea water taken equal to $\rho = 1025\,\mathrm{kg\,m^{-3}}$, g is the acceleration due to gravity, E is the spectral energy density distributed over frequencies f, and c_g is the group velocity. As the area of interest is characterized by important water depths with restricted extend of the continental shelf, we adopted the formulation of the group velocity in deep water $c_g = g/(4\pi f)$ resulting in the following relationship

$$P = \frac{\rho g^2}{4\pi} \int_0^\infty \frac{E(f)}{f} df \ . \tag{2}$$

The available wave power per unit crest is thus expressed as a function of the significant wave height $H_s = 4\sqrt{m_0}$ and the wave energy period $T_e = m_{-1}/m_0$ as

$$P = \frac{\rho g^2}{64\pi} H_s^2 T_e \tag{3}$$

with $m_n = \int_0^\infty f^n E(f) df$ the n^{th} order spectral moment. This formulation was traditionally implemented in numerical assessments of the wave resource [2, 34, 35, 36, 37]. Further details about the mathematical development of this formulation can also be found in [38] and [39]. Assuming a standard JONSWAP spectrum with a peak enhancement $\gamma = 3.3$, the mean wave period was estimated from the available peak period as $T_e = \alpha T_p$ with $\alpha = 0.9$ [4, 25, 40, 41]. It was thus possible to compute the available wave energy flux with integrated wave parameters , H_s and T_p, extracted from the wave hindcast database. However, differences may exist between this formulation based on integrated wave parameters and the available power computed

from spectral wave density, especially in cases of combined swell and wind seas [24]. These differences were disregarded here to be consistent with previous numerical estimations of the available wave energy flux covering the area of interest [2, 3, 13, 22, 23, 25]. It should furthermore be noted that such approximation will have reduced effects on the evaluation of the spatio-temporal variability of P that will mainly focus on the evolution of relative quantities.

3.3. Wave energy metrics

Following the studies of Cornett [2] at the worldwide scale and Gonçalves et al. [42] in the western French coast, a series of four metrics was considered to characterize the temporal variability of the available wave energy flux at monthly, seasonal and annual time scales: the coefficient of variation (COV), the seasonal variability index (SV), the monthly variability index (MV), and the annual variability index (AV). The coefficient of variation evaluates, at all time scales from hourly to annual, the amount of variability with respect to the mean value by dividing the standard deviation of P (σ_P) to the mean available wave power (P_{year}) over the 31-year period between 1979 and 2009

$$\mathrm{COV} = \frac{\sigma_P}{P_{year}} \ . \tag{4}$$

The seasonal variability index is defined as

$$\mathrm{SV} = \frac{P_{S1} - P_{S2}}{P_{year}} \tag{5}$$

where P_{S1} and P_{S2} are, over the multi-decadal time period considered, the mean available wave powers for the most and the least energetic seasons, respectively. The four seasons are defined with respect to three-month seasonal

time scale. Winter refers to the months of December, January and February; Spring to the months of March, April and May; Summer to the months of June, July and August; and Fall to the months of September, October and November.

The monthly and annual variability indexes are computed with similar formulations as:

$$\mathrm{MV} = \frac{P_{M1} - P_{M2}}{P_{year}} \tag{6}$$

and

$$\mathrm{AV} = \frac{P_{A1} - P_{A2}}{P_{year}} \tag{7}$$

where P_{M1} and P_{M2} are the mean powers for the most and the least energetic months, respectively; and P_{A1} and P_{A2} are the mean wave powers for the most and the least energetic years, respectively.

4. Results and discussion

4.1. Evaluation of the wave hindcast database

The hindcast database was evaluated in terms of significant wave height and peak period by the NCEP [28] (Section 3.1). These evaluations were here extended to the comparison of the available wave power from formulation 3, based on predictions and observations. Indeed, the approach of wave power can not be assessed from single evaluations of H_s and T_p as these two parameters do not have the same weight in the wave power formulation 3. This assessment was conducted in 41 NDBC wave buoys located in coastal and offshore waters with mean water depths over 40 m (Fig. 2). Historical observations of H_s and T_p were provided by the NDBC with a time step

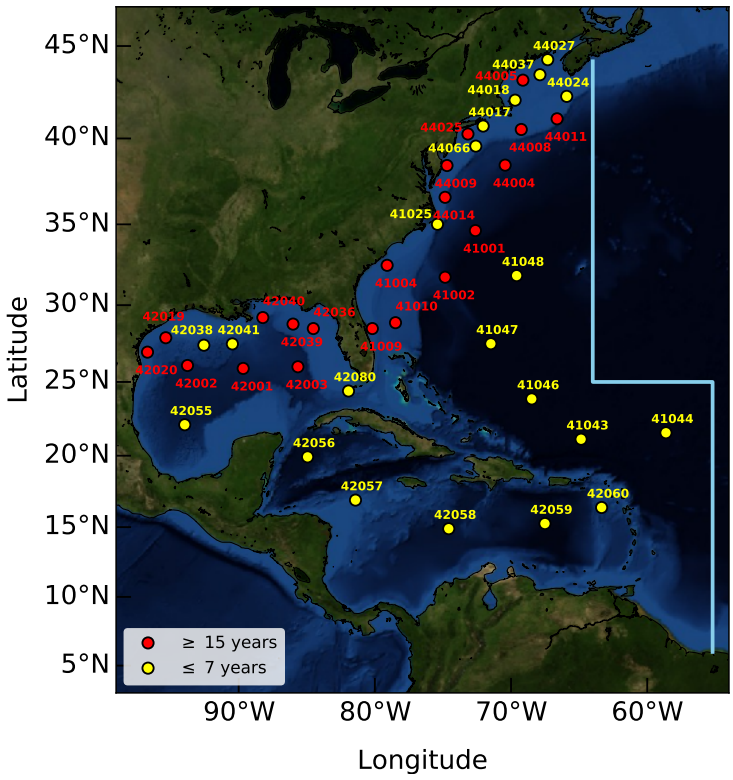

Figure 2: Locations of wave buoys considered for the assessment of the WWIII hindcast database displayed in red circles for long-term measurements ($\geq$ 15 years) and yellow circles for measurements on a shorter period ($\leq$ 7 years). The light blue line shows the outer limit of WWIII computational domain in the area of interest.

of one hour [19]. Whereas a water depth of 40 m may be at the limit of the application of formulation 3 based on the deep water assumption for the group velocity, such value extended the assessment of the database to coastal waters primary targeted for WEC implementation. Among the 41 wave buoys retained, 15 points were thus located in mean water depths below 150 m. The comparison between predictions and observations may furthermore be biased

by the duration period considered, whether this evaluation was established on several years or restricted to a few years. The available observations were thus characterized by different time periods with (i) 20 points covering more than 15 years and (ii) 21 points restricting to less than 7 years. The assessment of the wave hindcast database was thus performed with respect to these two categories. The associated spatial distribution highlighted very clearly the priority given to the observations in coastal waters along the USA East Coast (Fig. 2).

In order to provide simple overviews of the comparison between predicted and observed wave powers, the evaluation of the wave hindcast database was performed with Taylor diagrams [43] that incorporated the basic statistical measures of (i) the Pearson correlation coefficient

$$\mathrm{Pe} = \frac{1}{N} \frac{\sum_{i=1}^{i=N} (x_i - \bar{x})(y_i - \bar{y})}{\sigma_{obs}\sigma_{pred}} \ , \tag{8}$$

(ii) the Centered Root-Mean-Squared Difference

$$\mathrm{CRMSD}^2 = \frac{1}{N} \sum_{i=1}^{i=N} \left[(x_i - \bar{x}) - (y_i - \bar{y}) \right]^2 \tag{9}$$

and (iii) the standard deviations of observations and predictions

$$\sigma_{obs}^2 = \frac{1}{N} \sum_{i=1}^{i=N} (x_i - \bar{x})^2 \tag{10}$$

and

$$\sigma_{pred}^2 = \frac{1}{N} \sum_{i=1}^{i=N} (y_i - \bar{y})^2 \tag{11}$$

where N is the number of data in the discretised time series considered, (x_i) and (y_i) represent the two sets of measured and simulated values, and $\bar{x}$ and $\bar{y}$ are the mean values of observed and modelled data, respectively. CRMSD

satisfies the fundamental relationship at the basis of Taylor diagram construction [43] $\mathrm{CRMSD}^2 = \sigma_{obs}^2 + \sigma_{pred}^2 - 2\sigma_{obs}\sigma_{pred}\mathrm{Pe}$. Following Spindler et al. [44], σ_{obs}, σ_{pred} and CRMSD were normalized by σ_{obs} to display the assessment of the wave database in single plots with respect to the observations. Whereas conducted in different locations, observations were thus appearing on the same Taylor diagram as a point with Pearson correlation coefficient and normalized standard deviation equal to 1, and normalized CRMSD set to 0 (Fig. 3). In this case, the relative skill of predictions at wave buoys may be investigated from the values of statistical parameters between the point on Taylor diagram and the point of observation which keeps an unique position for the different evaluations.

As exposed by formulation 3, the evaluation of the available wave energy

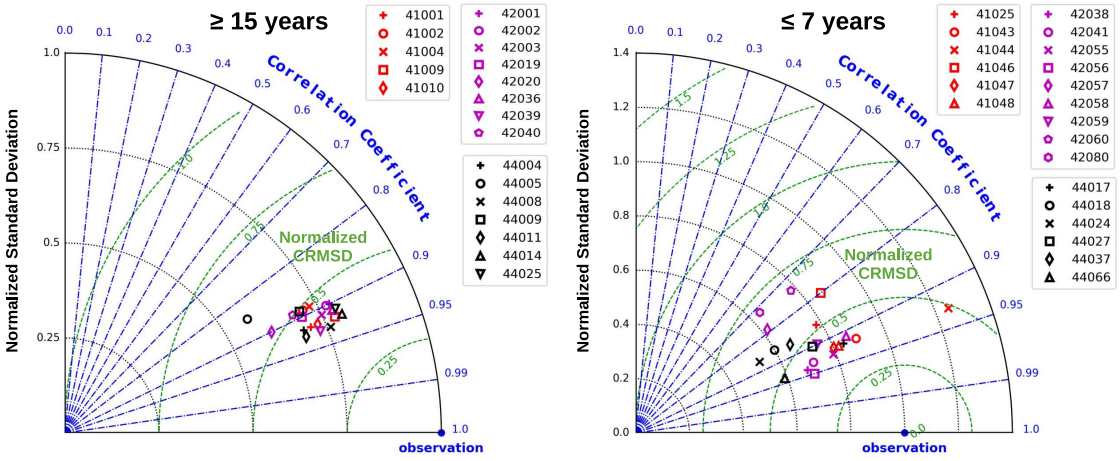

Figure 3: Taylor diagram of the estimation of the available wave energy flux P in NDBC wave buoys. The evaluation draws the line between observations that cover (left) more than 15 years and (right) less than 7 years. The point corresponding to observations is denoted as a blue circle on these figures.

flux depends more on the significant wave height (which is squared) than on the peak period. Whereas increased differences were obtained for the approach of the peak period [28, 44], a better agreement was thus reached here for the wave power density in relation to improved evaluations of the significant wave height (Fig. 3). With local exceptions for points 42020 and 44005 located close to the coastline, the evaluation of P from long-term observations ($\geq$ 15 years) showed reduced dispersion of statistical parameters in the Taylor diagram. For most of these points, the normalized CRMSD remained below 0.5 with correlation coefficient Pe over 0.89. The evaluation from measurements covering less than 7 years exhibited, however, a greater dispersion of points in the Taylor diagram with a series of locations characterized by normalized CRMSD over 0.5. Nevertheless, with exceptions for points 41046 and 41044 near the southern open boundary of computational domain, this concerned mainly locations in the vicinity of coastal irregularities such headlands or straits (42080, 44018, 44024, 44037) and in the wake of islands (42057 and 42060). While refined spatial resolutions may be adopted to capture these complex geometries and improve wave predictions, this may also increase dramatically the computational time required to construct the wave hindcast database.

Times series of observed and predicted wave power density confirmed finally the reliability of predictions for approaching the wave climate variability in offshore waters of the North-West Atlantic (41048), the GoM (42001) and the CS (42058) (Fig. 4). These comparisons revealed yet a tendency of predictions to underestimate peak values of P, typically in storm conditions. However, taking into account the fact that WEC stopped operating under a

high sea state (survival mode), reduced effects were expected on characterizing the temporal variabilities of energy output at a given location.

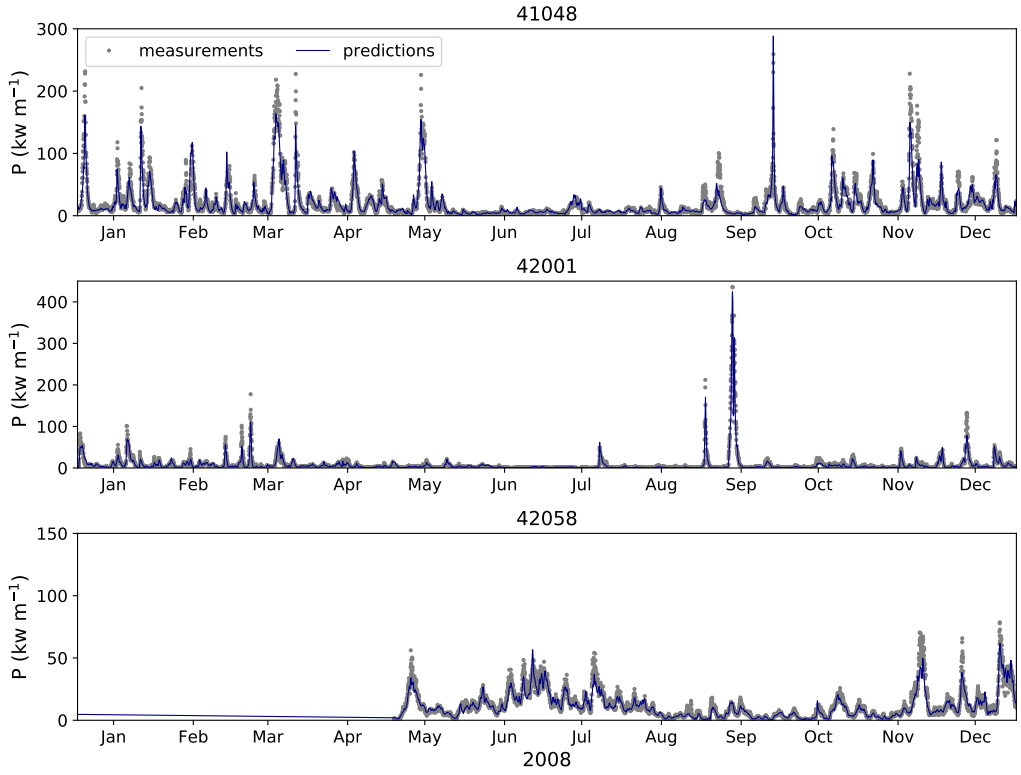

Figure 4: Time series of observed and predicted available wave energy flux at wave buoys 41048, 42001 and 42058 in 2008.

4.2. Spatial distribution of wave energetic patterns

Confirming previous numerical investigations of the available wave power density in the European continental shelf seas [9, 45], a close correlation was exhibited between the averaged significant wave height and the available wave energy flux (Fig. 5). The northern oceanic region off the USA East Coast was thus characterized by the most energetic conditions of the area

of interest with mean wave height over 2.2 m and wave power density over 28 kWm^{-1}. This evaluation was consistent with worldwide assessments of the mean available wave power density that estimated the wave energy resource between 20 and 30 kWm^{-1} in these offshore regions [2, 3, 22, 23]. Off the North-East Coast of USA, the computed mean wave power was in the range of values obtained by Defne et al. [24] from the exploitation of wave buoys observations with available wave energy fluxes of 17.5 kWm^{-1} at point 41001 and 6.9 kWm^{-1} at point 41004. Being less exposed to ocean waves, the GoM and CS areas were characterized by reduced energetic conditions. In these two regions, the estimation of the wave power resource was consistent with the numerical investigations conducted by Appendini et al. [13]

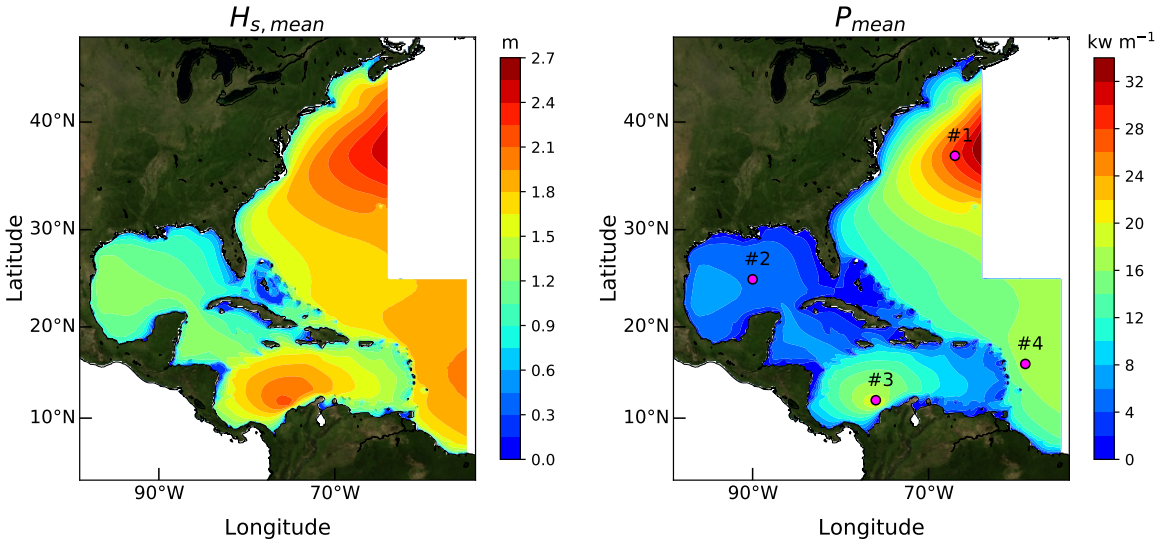

Figure 5: Predicted averaged significant wave height $H_{s,mean}$ and available wave energy flux P_{mean} over the period 1979-2009. Points #1 to #4 selected for the analysis of time series of available wave power density are shown with magenta circles.

which resulted in mean values of P up to 13 $\mathrm{kWm^{-1}}$ in the CS (off Colombia) and below 8 $\mathrm{kWm^{-1}}$ in the GoM. However, an area of high available wave power density was identified in the CS off Colombia, with energy levels comparable to the southern oceanic region off the Lesser Antilles. As exhibited by Appendini [13], this wave energy pattern was mainly associated to the influence of an easterly zonal wind, liable to reach 13 $\mathrm{m\,s^{-1}}$ and known as the Caribbean Low-Level Jet (CLLJ).

4.3. Temporal variability of wave energy

However, integrated parameters such as the mean available wave energy flux provided limited information for a refined evaluation of the technically exploitable energy [3]. The temporal variability of the available resource was thus investigated at the monthly time scale exhibiting a clear contrast between (i) winter months with the highest energetic conditions and (ii) summer months with reduced energy levels (Fig. 6). The spatial distributions of wave energetic patterns at the seasonal scale confirmed these temporal variations (Fig. 7). In accordance with simulations performed by Allahdadi et al. [27], a significant decrease of the available wave power was revealed along the USA East Coast between the winter and the summer periods. The averaged yearly time series (Fig. 6) may be, very roughly, compared with waves conditions in the North-East Atlantic along the European shelf seas [6, 9, 10] that exhibited increased inter-annual power variabilities in the most energetic locations. Areas such as the CS showed, however, summer waves energetic conditions comparable to winter energy levels with values of P over 25 $\mathrm{kWm^{-1}}$. These differences were exhibited in four locations (#1 to #4) that characterized the wave climate in different sub-regions of the area of interest (Figs. 5 and

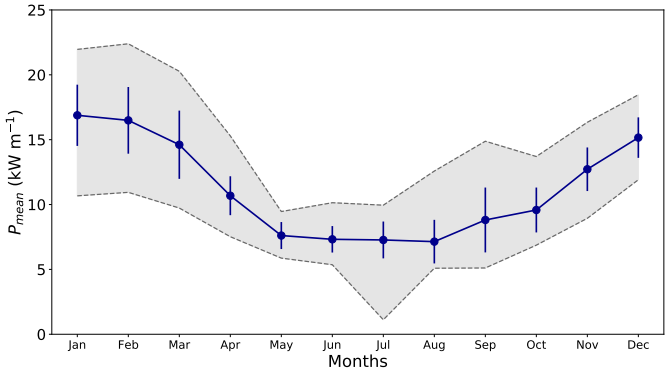

Figure 6: Yearly time series of the averaged predicted available wave energy flux over the WWIII computational domain and the period 1979-2009. Errors bars show the associated standard deviation while grey shading indicates the range of numerical values.

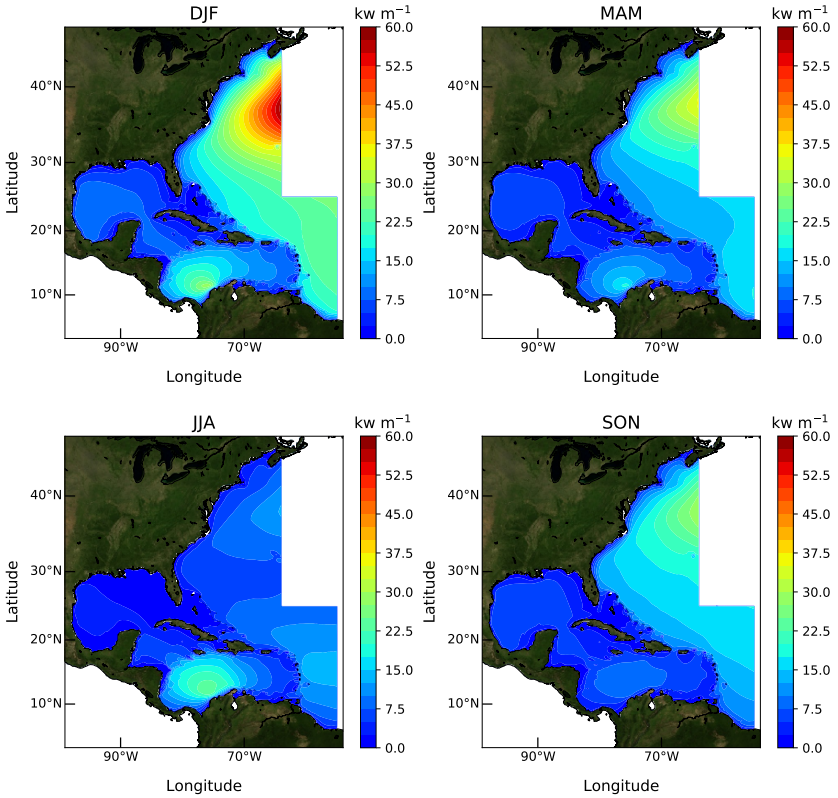

Figure 7: Seasonal evolutions of mean available wave energy flux predicted over the period 1979-2009.

8, and Tab. 1). In comparison with the oceanic regions (points #1 and #4) and the GoM (point #2), the evolution of the wave climate in the CS (point #3) was thus characterized by two peaks in February and July that resulted from the CLLJ [13]. In the GoM (point #2), significant variability of the available resource was furthermore exhibited between August and November in relation to the influence of tropical cyclones with the biggest impact on September [21, 25]. Whereas appearing in semi-enclosed basins with reduced energy levels, these temporal variations impacted the value of predicted available wave power averaged over the WWIII computational domain and the 31-year period between 1979 and 2009 (Fig. 6).

The spatial heterogeneity in the temporal variability of the wave climate was evaluated with the four statistical metrics COV, SV, MV, and AV (Section 3.3) (Fig. 9). The results, obtained from the exploitation of the wave hindcast database, appeared consistent with the worldwide assessment of wave power variability [2, 23] with a coefficient of variation exceeding 2.5 in the GoM, seemingly associated with the influence of tropical cyclones. The SV and MV indexes followed also the spatial distribution established by Cornett [2] in spite of slight differences for MV in the south-eastern part of the GoM. Our local investigation of wave power variability was also consistent with results obtained by Appendini et al. [13] in the southern CS with values of COV and SV restricted to 0.8 and 1.0, respectively. The spatial distribution of these statistical metrics highlighted that the temporal variability in wave power was not the same everywhere, and established differently at monthly, seasonal and annual time scales. In the oceanic regions of the North-West Atlantic, a clear contrast was thus exhibited between (i)

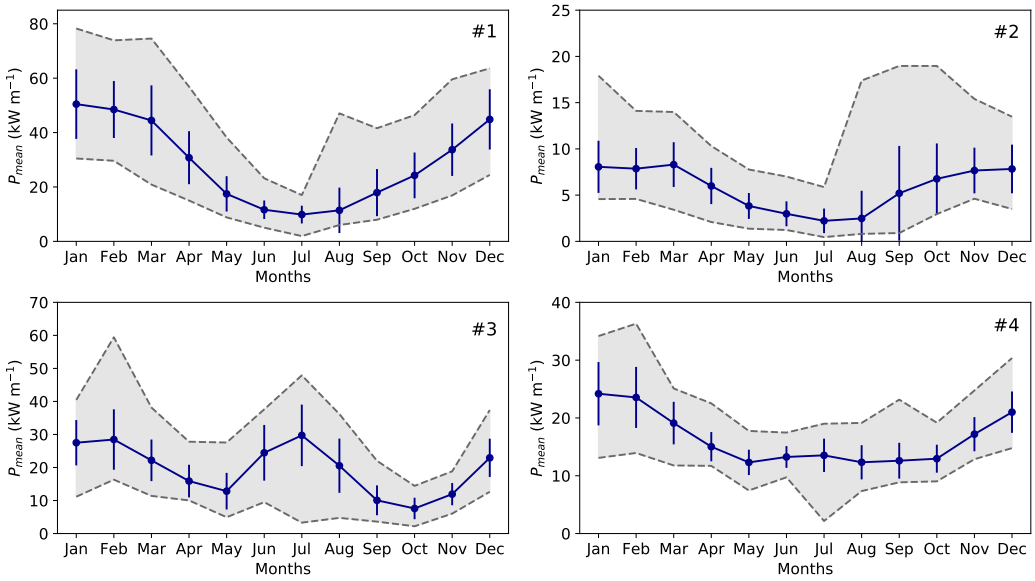

Figure 8: Yearly time series of the averaged predicted available wave energy flux over the period 1979-2009 at locations #1 to #4. Errors bars show the associated standard deviation while grey shading indicates the range of numerical values.

Table 1: Statistical metrics for wave energy conditions at locations #1 to #4 with the water depths and the mean available wave energy flux P_{mean} over the 31-year period considered.

Points	Coordinates		Water depths	P_{mean}	COV	SV	MV	AV
	Lon.	Lat.	(m)	(kWm^{-1})				
#1	67° W	37° N	4999	28.7	0.6	1.3	1.4	0.4
#2	90° W	25° N	3536	5.7	0.6	0.9	1.0	0.5
#3	76° W	12° N	3296	19.5	0.5	0.8	1.1	0.6
#4	59° W	16° N	5204	16.4	0.3	0.6	0.7	0.3

348 the northern energetic area (off the USA East Coast) with significant tempo-
349 ral variability and (ii) the southern part (off the Greater and Lesser Antilles)
350 with reduced energy levels and variability. This difference was also high-
351 lighted by the time series of the averaged predicted available wave power
352 density at points #1 and #4 (Fig. 8). In spite of reduced energy levels, the
353 wave power resource was finally particularly unsteady in the GoM in relation

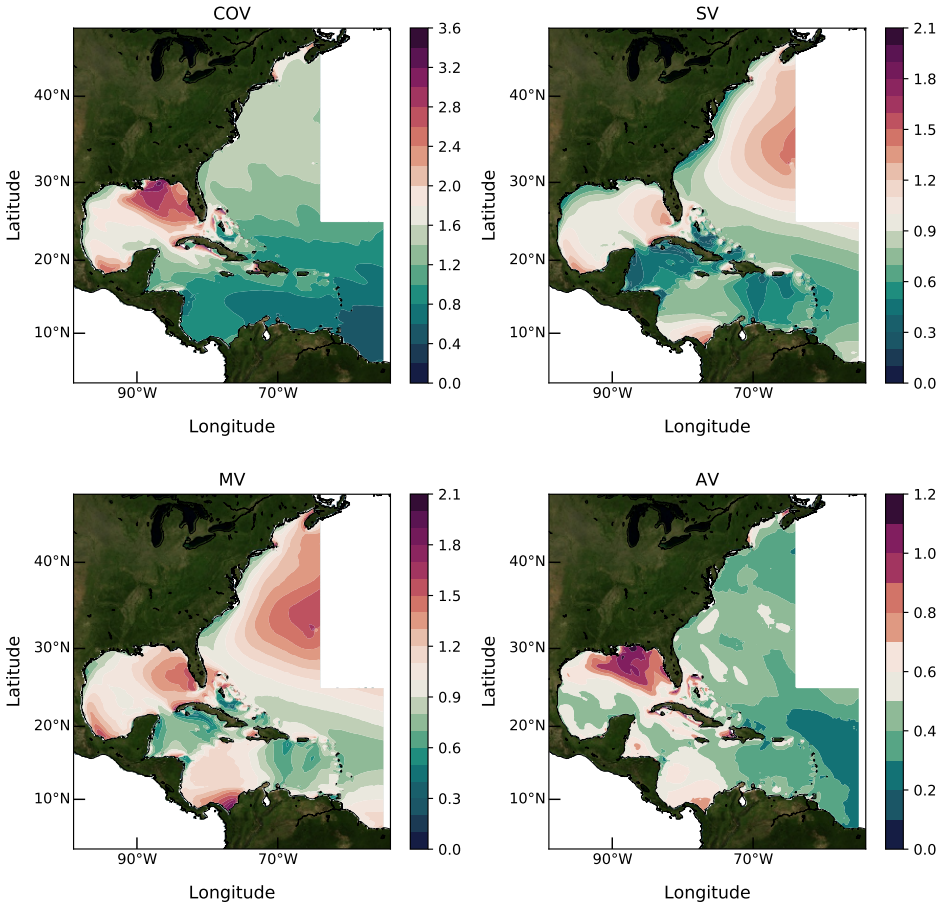

Figure 9: Temporal variability indexes of the available wave energy flux between 1979 and 2009.

to the influence of multiple hurricanes. While reduced in comparison to the GoM, the south-western part of the CS showed also temporal variability particularly noticeable at monthly time scale and seemingly associated to the influence of the CLLJ. The AV index exhibited finally a zonation between (i) the oceanic regions and the CS where it was restricted to 0.7 and (ii) the GoM where it exceeded 1.0 (Fig. 9).

4.4. Comparative analysis of wave energy extraction scenarios

A comparative analysis was conducted to investigate the theoretical extractable energy in locations #1 to #4 characterized by varying wave climates. However, the energy output was, most of the time, determined with respect to the technological characteristics and performances of the device, by relying, for instance, on the power matrix that provided the power generated in different classes of wave height and period (see [4] for a non-exhaustive review). Whereas this approach resulted in a refined quantification of the energy output (particularly useful for preliminary studies of WEC implementation in the marine environment), results obtained were dependent from the device technology restricting the scope of these studies.

In the present investigation, we followed instead the generic approach proposed by Portilla et al. [3] which provided a comparative analysis of wave power exploitation by introducing variables independent from the device and expressed in units of power over units of distance (in Wm^{-1}). This study considered a series of variables commonly used in WEC resource assessments: (i) the installed capacity (IC), (ii) the nominal installed capacity (NC), (iii) the annual electricity production (AP) and (iv) the capacity factor (CF). The installed capacity (expressed in Wm^{-1}) refers to the amount of energy

that would be produced by WEC operating at its full capacity. The nominal installed capacity (expressed in $\mathrm{Whm^{-1}year^{-1}}$) quantifies thus the total energy produced during a given period of time (typically one year) if the device operates at its full IC. The annual electricity production (expressed in $\mathrm{Whm^{-1}year^{-1}}$) is the total energy produced by the device during a year. The capacity factor (with no units) refers finally to the performance of the device by accounting for the fraction of the time the energy converter is operating at full capacity. It is defined as the ratio between AP and NC. Following Portilla et al. [3], we considered finally two energy extraction scenarios at the four locations #1 to #4. In the first scenario A, WEC were converted the available wave energy flux with the upper limit of the IC. In the second scenario B, more realistic operation conditions were introduced. WEC were thus operated above a given threshold of available energy and were halted below too strong wave conditions to guarantee the protection of the device and enter into survival mode. Portilla et al. [3] considered three levels of lower and upper limits at 10, 20 and 30%, respectively. However, their investigation was restricted to two locations in the North Atlantic and the Equatorial Pacific. As we considered here four locations, the analysis was simplified by retaining the mid-value of 20%, setting the lower and upper limits at 20 and 120% of the IC, respectively.

In scenario A, as expected, the annual electricity production (computed over the 31-year period) was growing with the installed capacity reaching a limit when the IC exceeded the available resource while the capacity factor was decreasing by increasing IC and the nominal installed capacity (Fig. 10). The IC of a device has thus to be adapted to the local wave climate to guaran-

tee the balance between a minimum amount of energy output and high WEC performances. This aspect is fundamental as increasing the IC of a device requires significant capital investments which reduces the economical yield and profitability of a wave energy farm. In the present investigation, low installed capacity had thus to be considered in the low energetic location #2 of the GoM whereas extra capacity for power generation still existed in the energetic point #1 of the North-West Atlantic, but with reduced CF. However, this evaluation may be influenced by the wave power variability. Whereas the mean available wave energy flux P_{mean} was 75% higher at point #1 than point #4 (Tab. 1), the annual production and the capacity factor may be lower in the northern oceanic region (point #1) than in its southern part (point #4). For IC = 18 kWm^{-1}, AP was thus estimated at 108 kWhm^{-1}year^{-1} at point #1 against 117 kWhm^{-1}year^{-1} at point #4, and CF was computed at 0.68 at #1 against 0.74 at #4. The high wave power variability at point #1,

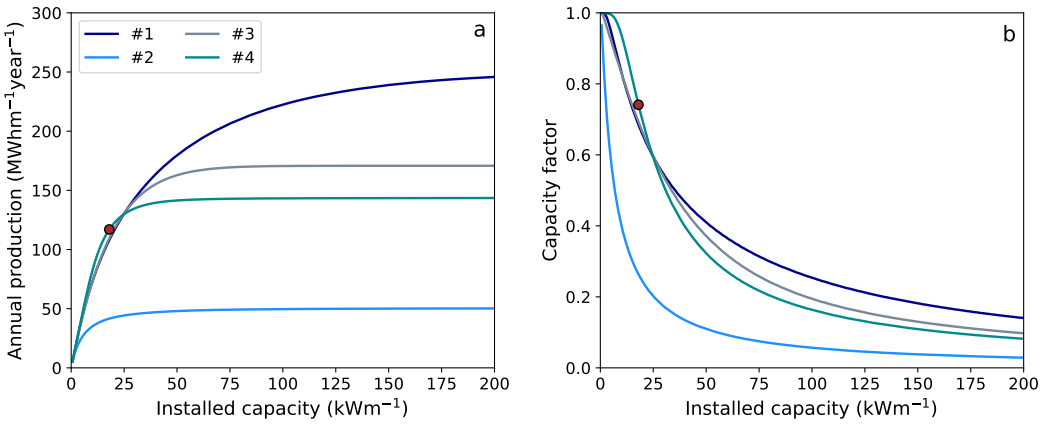

Figure 10: Predicted (a) annual production and (b) capacity factor against the installed capacity at locations #1 to #4 for the first case study A. The brown circle indicates the reference taken to illustrate the comparison between the four locations.

exhibited by the statistical metrics, (Tab. 1 and Section 4.3) may explain these differences. Indeed, at point #1, the energy produced during storm events was restricted to reduced IC whereas it may be dramatically lower during summer calm weather conditions (Fig. 8). This energy production contrasted with the output at point #4 where more regular wave conditions were approaching, for low IC, the nominal installed capacity increasing WEC performances.

In scenario B, the analysis confirmed results obtained by Portilla et al. [3] that exhibited peak values for AP and CF with respect to the installed capacity IC (Fig. 11). Indeed, as expected, the annual production reached a peak value when the IC range (between the lower and upper limits of the operation of the device) captured the maximum available wave resource. WEC with reduced IC harnessed thus the lower part of the available wave energy while devices with high IC failed to operate at full capacity. However, the

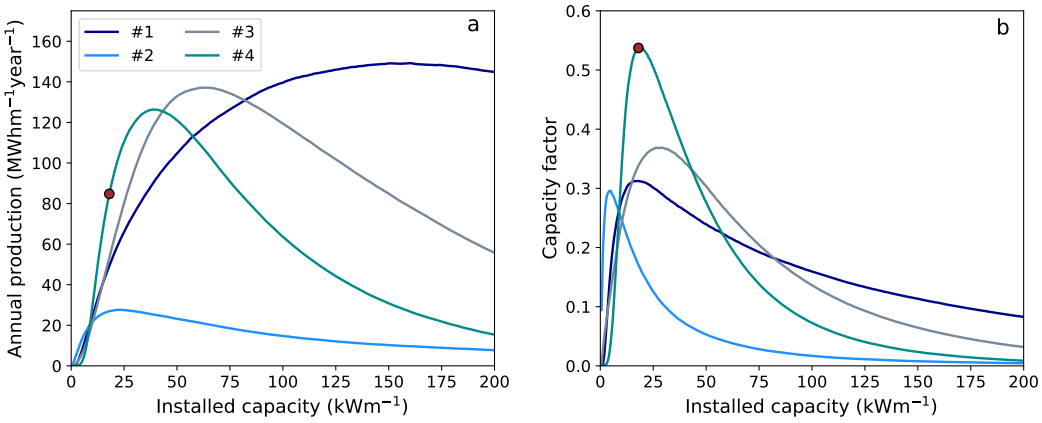

Figure 11: Predicted (a) annual production and (b) capacity factor against the installed capacity at locations #1 to #4 for the second case study B. The brown circle indicates the reference taken to illustrate the comparison between the four locations.

peaks of AP and CF were not reached for the same IC at a given location. Indeed, as exhibited in scenario A, reduced AP may be reached with high WEC performances and CF. Moreover, the introduction of start-up and survival mode conditioned the adaptability of WEC to a given wave climate. At the four locations considered, this resulted in differences between the optimal values of IC that provided the maximum AP or CF. For IC = 18 kWm^{-1}, we exhibited thus the optimal values of CF at point #4 (CF=0.54) whereas reduced CF were obtained at the energetic location #1 (CF=0.31).

In both configurations, site #2, located in the GoM, presented limited interest for the setup of wave energy converters being characterized by reduced AP and CF. In spite of oceanic energetic conditions, site #1, off the USA East Coast, required increased IC, with high capital investments, to provide AP comparable to the values obtained at sites #3 and #4, in the CS and off the Lesser Antilles (Fig. 11-a). These two locations appeared finally interesting for the exploitation of the wave energy showing (i) moderated energetic conditions compatible with WEC operations and (ii) moderated variability of the energy resource in comparison with the northern oceanic region or the GoM (Section 4.3). Site #4 was particularly attractive reaching the highest CF values at low IC (Fig. 11-b) and being located off energy starved territories of the Lesser Antilles (Fig. 5).

5. Conclusions

A 31-year consistent wave hindcast database was exploited to provide detailed insights into the temporal variability of the available wave energy resource and its exploitation by WEC in the region covering the North-West

Atlantic, the GoM and the CS. Complementing previous evaluations based on the significant wave height and the peak period, the database was assessed by comparing the available wave energy flux, derived from predictions and observations, in 41 buoys located in coastal and offshore waters of the area of interest. In addition to a map of averaged wave energetic patterns, a series of four metrics was considered to exhibit the temporal variability of the resource at monthly, seasonal and annual time scales. A generic method was finally applied to characterize the theoretical exploitable energy in four locations with varying wave climates. The main outcomes of the present study are as follows:

1. A clear contrast was exhibited in the available wave energy flux between the oceanic regions of the North-West Atlantic and the semi-enclosed basins, protected from incoming waves conditions by a series of islands. However, a localized region with high wave power density was identified in the CS, off Colombia, within the area of influence of the Caribbean Low-Level Jet.
2. The exploitation of the hindcast database revealed differences in the yearly time series of the averaged predicted available wave power between the northern and southern parts of the North-West Atlantic, the GoM, and the CS. The northern oceanic regions exhibited thus a clear contrast between (i) the winter energetic conditions and (ii) the summer low-energetic period. However, this evolution contrasted with the wave climate in the CS that exhibited two peak values of the available wave power during the months of February and July in relation to the influence of the CLLJ.

3. Varying temporal variabilities of the available wave energy flux were exhibited by the four statistical metrics COV, SV, MV, and AV. Whereas the northern oceanic area showed significant temporal variability during the energetic winter period, the southern region, off the Lesser Antilles, displayed reduced temporal variations at the monthly, seasonal and annual time scales. The wave power resource was particularly unsteady in the GoM in relation to the influence of multiple hurricanes and was characterized by monthly variability in the south-western CS. A clear zonation was also identified at the annual time scale between the CS and the oceanic regions where it was reduced and the GoM where it was pronounced.
4. The comparative analysis of wave energy extraction scenarios revealed the reduced interest of the GoM for the exploitation of the wave energy. The results obtained confirmed furthermore that less energetic, but with more regular waves conditions (such as the CS and the southern oceanic region off the Lesser Antilles) may provide energy output levels comparable to the classically high-energetic ocean regions characterized by significant temporal variability (such as the northern oceanic area). The region off the Lesser Antilles appeared particularly interesting for WEC implementation to supply, at reduced installed capacity, a part of sustainable marine renewable energies within the electricity grid of island territories.

The exploitation of a long-term wave hindcast database provided potential developers and government further insights about the temporal variability of the available wave energy flux and its exploitation in a region char-

acterized by varying wave climate conditions. The present investigation will undeniably benefit from broader exploitation of hindcast database in the most promising locations for the exploitation of the wave energy around the world. The results obtained may furthermore serve as a background reference for the implementation of advanced numerical simulations of the waves conditions and the available wave power in the area of interest. These refined assessments will naturally help to optimize the design and locations of WEC in nearshore coastal waters with advanced estimations of the associated energy output.

Credit author statement

Nicolas Guillou: Conceptualization, Methodology, Software, Validation, Formal analysis, Investigation, Writing Original Draft, Writing Review & Editing, Visualization, Supervision. **Georges Chapalain:** Writing Review & Editing.

Acknowledgements

In-situ observations and predicted wave data were provided by the National Oceanic and Atmospheric Administration (NOAA). The present paper is a contribution to the research program DIADEME ("Design et InterActions des Dispositifs d'extraction d'Energie Marine avec l'Environnement") (part dedicated to the Lesser Antilles area) of the Laboratory of Coastal Engineering and Environment (Cerema, http://www.cerema.fr).

References

[1] SI Ocean, Wave and tidal energy market deployment strategy for Europe, Intelligent Energy Europe Programme of the European Union, SI Ocean, 2014.

[2] A. Cornett, A global wave energy resource assessment, in: Proceedings of the International Journal of Offshore and Polar Engineering, 2008.

[3] J. Portilla, J. Sosa, L. Cavaleri, Wave energy resources: Wave climate and exploitation, Renewable Energy 57 (2013) 594–605.

[4] N. Guillou, G. Chapalain, Annual and seasonal variabilities in the performances of wave energy converters, Energy 165 (2018) 812–823.

[5] EPRI, Mapping and Assessment of the United States Ocean Wave Energy Resource, Technical Report 1024637, Electric Power Research Institute, 2011.

[6] S. Neill, M. Hashemi, Wave power variability over the northwest European shelf seas, Applied Energy 106 (2013) 31–46.

[7] S. Gallagher, R. Tiron, F. Dias, A long-term nearshore wave hindcast for Ireland: Atlantic and Irish Sea coasts (1979-2012), Ocean Dynamics 64 (2014) 1163–1180.

[8] S. Neill, M. Lewis, M. Hashemi, E. Slater, J. Lawrence, S. Spall, Inter-annual and inter-seasonal variability of the Orkney wave power resource, Applied Energy 132 (2014) 339–348.

[9] N. Guillou, G. Chapalain, Numerical modelling of nearshore wave energy resource in the Sea of Iroise, Renewable Energy 83 (2015) 942–953.

[10] N. Guillou, Evaluation of wave energy potential in the Sea of Iroise with two spectral models, Ocean Engineering 106 (2015) 141–151.

[11] B. R. D. Robertson, C. E. Hiles, B. J. Buckham, Characterizing the near shore wave energy resource on the west coast of Vancouver Island, Canada, Renewable Energy 71 (2014) 665–678.

[12] J. Sierra, C. Martina, C. Mössoa, M. Mestres, R. Jebbada, Wave energy potential along the Atlantic coast of Morocco, Renewable Energy 96(A) (2016) 20–32.

[13] C. Appendini, C. Urbano-Latorre, B. Figueroa, C. Dagua-Paz, A. Torres-Freyermuth, P. Salles, Wave energy potential assessment in the Caribbean Low Level Jet using wave hindcast information, Applied Energy 137 (2015) 375–384.

[14] Z. Wang, C. Duan, S. Dong, Long-term wind and wave energy resource assessment in the South China sea based on 30-year hindcast data, Ocean Engineering 163 (2018) 58–75.

[15] J. Morim, N. Cartwright, A. Etemad-Shahidi, D. Strauss, M. Hemer, Wave energy resource assessment along the Southeast coast of Australia, Applied Energy 184 (2016) 276–297.

[16] E. Kirinus, P. Oleinik, J. Costi, W. Marques, Long-term simulations for ocean energy off the Brazilian coast, Energy 163 (2018) 364–382.

[17] M. Love, A. Baldera, C. Yeung, C. Robbins, The Gulf of Mexico Ecosystem: A Coastal and Marine Atlas, Technical Report, LA: Ocean Conservancy, Gulf Restoration Center, 2013.

[18] NOAA, https://polar.ncep.noaa.gov/waves/hindcasts/, 2019.

[19] NDBC, https://www.ndbc.noaa.gov/historical_data.shtml, 2019.

[20] C. Appendini, A. Torres-Freyermuth, F. Oropeza, P. Salles, J. López, E. T. Mendoza, Wave modeling performances in the Gulf of Mexico and Western Caribbean: Wind reanalyses assessment, Applied Ocean Research 39 (2012) 20–30.

[21] A. Devis-Morales, R. A. Montoya-Sánchez, G. Bernal, A. F. Osorio, Assessment of extreme wind and waves in the Colombian Caribbean Sea for offshore applications, Applied Ocean Research 69 (2017) 10–26.

[22] K. Gunn, C. Stock-Williams, Quantifying the global wave power resource, Renewable Energy 44 (2012) 296–304.

[23] B. Reguero, I. Losada, F. Méndez, A global wave power resource and its seasonal, interannual and long-term variability, Applied Energy 148 (2015) 366–380.

[24] Z. Defne, K. A. Haas, H. M. Fritz, Wave power potential along the Atlantic coast of the southeastern USA, Renewable Energy 34 (2009) 2197–2205.

[25] F. Haces-Fernandez, H. Li, D. Ramirez, Wave energy characterization

591 and assessment in the U.S. Gulf of Mexico, East and West Coasts with
592 Energy Event Concept, Renewable Energy 123 (2018) 312–322.

593 [26] S. Ortega, A. F. Osorio, P. Agudelo, Estimation of the wave power
594 resource in the Caribbean Sea in areas with scarce instrumentation. Case
595 study: Isla Fuerte, Colombia, Renewable Energy 57 (2013) 240–248.

596 [27] M. N. Allahdadi, B. Gunawan, J. Lai, R. He, V. S. Neary, Development
597 and validation of a regional-scale high-resolution unstructured model for
598 wave energy resource characterization along the US East Coast, Renew-
599 able Energy 136 (2019) 500–511.

600 [28] NCEP, WAVEWATCH III 30-year Hindcast Phase 2, https://polar.
601 ncep.noaa.gov/waves/hindcasts/nopp-phase2.php, 2019.

602 [29] H. Tolman, User manual and system documentation of WAVEWATCH-
603 III version 3.14, Tech. Rep., NOAA/NWS/NCEP/MMAB, 2009.

604 [30] F. Ardhuin, E. Rogers, A. Babanin, J.-F. Filipot, R. Magne, A. Roland,
605 A. van der Westhuysen, P. Queffeulou, J.-M. Lefevre, L. Aouf, F. Col-
606 lard, Semi-empirical dissipation source functions for wind-wave mod-
607 els. Part I: Definition, calibration, and validation., Journal of Physical
608 Oceanography 40 (2010) 1917–1941.

609 [31] A. Chawla, D. Spindler, H. Tolman, WAVEWATCH III Hindcasts with
610 Re-analysis winds. Initial report on model setup, Technical Report, Na-
611 tional Oceanic and Atmospheric Administration, 2011.

612 [32] A. Chawla, D. Spindler, H. Tolman, 30 Year Wave Hindcasts using

WAVEWATCH III with CFSR winds - Phase 1, Technical Report, National Oceanic and Atmospheric Administration, 2012.

[33] Saha et al., The NCEP Climate Forecast System Reanalysis, Bull. Am. Meteor. Soc. (2010) 1015–1057.

[34] R. Waters, J. Engström, J. Isberg, M. Leijon, Wave climate off the Swedish west coast, Renewable Energy 34 (6) (2009) 1600–1606.

[35] G. Iglesias, R. Carballo, Wave energy potential along the Death Coast (Spain), Energy 34 (2009) 1963–1975.

[36] D. Vicinanza, P. Contestabile, V. Ferrante, Wave energy potential in the north-west of Sardinia (Italy), Renewable Energy 50 (2013) 506–521.

[37] M. Gonçalves, P. Martinho, C. G. Soares, Assessment of wave energy in the Canary Islands, Renewable Energy 68 (2014) 774–784.

[38] A. Pecher, J. P. Kofoed, Handbook of Ocean Wave Energy, Springer Open, 2017.

[39] S. Neill, M. Hashemi, Fundamentals of Ocean Renewable Energy - Generating Electricity from the Sea, Elsevier Academic Press, 2018.

[40] J. Pastor, Y. Liu, Wave Climate Resource Analysis Based on a Revised Gamma Spectrum for Wave Energy Conversion Technology, Sustainability 8 (1321) (2016) –.

[41] J. Sierra, A. White, C. Mösso, M. Mestres, Assessment of the intra-annual and inter-annual variability of the wave energy resource in the Bay of Biscay (France), Energy 141 (2017) 853–868.

[42] M. Gonçalves, P. Martinho, C. G. Soares, A 33-year hindcast on wave energy assessment in the western French coast, Energy 165 (2018) 790–801.

[43] K. E. Taylor, Summarizing multiple aspects of model performance in a single diagram, Journal of Geophysical Research 106 (2001) 7183–7192.

[44] D. M. Spindler, A. Chawla, H. L. Tolman, An initial look at the CFSR Reanalysis winds for wave modeling, Tech. Rep., Environmental Modeling Center - Marine Modeling and Analysis Branch, 2011.

[45] E. Rusu, C. G. Soares, Numerical modelling to estimate the spatial distribution of the wave energy in the Portuguese nearshore, Renewable Energy 34 (2009) 1501–1516.